https://doi.org/10.20965/ijat.2015.p0381

Paper:

Elimination of Gyro Drift by Using Reversal Measurement

Tatsuya Kume*, Masanori Satoh, Tsuyoshi Suwada**, Kazuro Furukawa**, and Eiki Okuyama*****

*Mechanical Engineering Centre, High Energy Accelerator Research Organization (KEK)
1-1 Oho, Tsukuba, Ibaraki 305-0801, Japan
E-mail: tatsuya.kume@kek.jp
**Accelerator Laboratory, High Energy Accelerator Research Organization (KEK)
1-1 Oho, Tsukuba, Ibaraki 305-0801, Japan
***Faculty of Engineering and Resource, Akita University
1-1 Tegata gakuen-machi, Akita 010-8502, Japan

[Received January 15, 2015; accepted June 17, 2015]

We aim to realize a large-scale straightness evaluation using a gyro. It detects tangential angles to evaluate a profile without any references. However, fluctuations of angular signal, called gyro drift, are considered a major contributor of error. We adopted a reversal measurement for eliminating the drift. The reversal measurement has been widely used for eliminating stable error from ancient. Here, we periodically performed reversal measurements for eliminating drift of a commercially available fiber optic gyro (FOG) unit. As a result, an angle could be derived with a standard deviation of 0.4 mrad for 1 hour of repeated measurements with an interval of 60 s, even though the gyro has a drift of several mrad/h including the effects of the Earth's rotation. This indicates that the reversal measurement is effective in reducing the drift.

Keywords: gyro, drift, rate offset, reversal measurement, straightness

1. Introduction

Large particle accelerators ranging in size from several hundred meters to several tens of kilometers have been operated and planned for advanced industrial applications and experiments for high energy physics [1–6]. Their components must be aligned with high accuracy to obtain their expected performance. It follows that their alignment should be evaluated with sufficient accuracy on the order of sub-mm or better for all dimensions in their primary mechanical alignment stage [7–11]. However, an evaluation accuracy better than 0.1 mm for an object larger than 100 m is fairly challenging [12, 13].

Straightness evaluation by detecting tangential angles of a profile [14–19] is considered advantageous for large objects because it is not affected by transferring locus of the straightness detector. The locus, usually used as a reference, should be defined accurately; however, it becomes difficult to maintain the accuracy over a long distance. We have evaluated the straightness of a 71-m-long section of our linear particle accelerator (linac) by using a precise inclinometer with a reproducibility of less than 49 μm [20]. We have also demonstrated the straightness evaluation for a distance up to 206 m and showed that this method is valid for evaluating large objects [21]. However, the method using an inclinometer can be applied only for evaluating straightness in a vertical plane because it uses the direction of gravity as a reference. It also introduces error caused by the Earth's roundness, which cannot be ignored when evaluating an object longer than 100 m with an accuracy better than 1 mm.

We aim to expand this method into the evaluation of straightness in the horizontal plane and to eliminate the error caused by the Earth's roundness. An autocollimator has been widely used for evaluating straightness without being affected by gravity [14, 16, 18, 19]; however, its evaluation distance is limited with a maximum length of approximately 100 m by its measurement beam range. On the other hand, gyros can detect angles without any references. It follows that gyros can detect angles without being affected by gravity and that they have no limitation in their evaluation distance. Furthermore, sensitive gyros can resolve angles on the order of μrads. However, even the most stable gyro has 0.01 deg/hour of fluctuation in its angular signal, which we call gyro drift or gyro rate offset. This value is not acceptable for detecting tangential angles with uncertainties smaller than several μrads, which is necessary for evaluating the straightness with an uncertainty smaller than 1 mm [20, 21].

Here, we adopt a reversal measurement [22] for eliminating the drift. The reversal measurement is usually used to eliminate stable error; however, we consider that its use can be expanded to eliminate drift by conducting the measurement at a sufficient rate to avoid drift changes and periodically to follow the drift change.

2. Principles

2.1. Reversal Measurement Using a Gyro

Figure 1 shows an analysis model for reversal measurements using a gyro. The gyro periodically turns π rad with an interval Δt around an axis perpendicular to

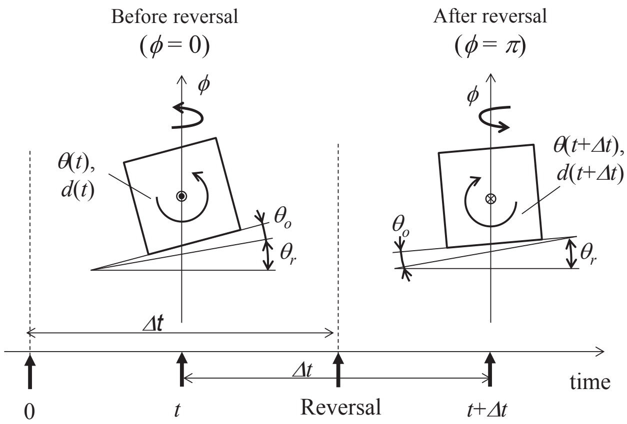

Fig. 1. Basic concept for eliminating the gyro drift by means of reversal measurements.

the gyro axis, around which the gyro is sensitive where ϕ is the gyro rotation angle. Angles $\theta(t)$ and $\theta(t+\Delta t)$ detected by the gyro at times t and $t+\Delta t$ before and after the reversal are expressed as:

$$\theta(t) = \theta_r + \theta_o + d(t) \quad \ldots \ldots \ldots \quad (1)$$

and

$$\theta(t+\Delta t) = -\theta_r + \theta_o + d(t+\Delta t), \quad \ldots \ldots \quad (2)$$

respectively. In these equations, θ_r and θ_o are the angles of the object and the offset angle of the gyro, respectively, and $d(t)$ and $d(t+\Delta t)$ are the gyro drift at times t and $t+\Delta t$, respectively.

The angle of the object θ_r can be derived by:

$$\theta_r = \frac{\theta(t) - \theta(t+\Delta t)}{2} - \frac{d(t) - d(t+\Delta t)}{2}. \quad \ldots \quad (3)$$

If the reversal is conducted at a sufficient rate compared to the drift, the difference $d(t) - d(t+\Delta t)$ converges to zero, and the angle to be measured θ_r will be obtained as:

$$\theta_r = \frac{\theta(t) - \theta(t+\Delta t)}{2}. \quad \ldots \ldots \ldots \quad (4)$$

This is the basic concept for eliminating the gyro drift by means of reversal measurements.

2.2. Effects of the Earth's Rotation

The Earth rotates once a day, which corresponds to an angular velocity (rate) ω of 73 μrad/s. This rotation cannot be ignored when detecting angles with a resolution of μrad. **Fig. 2** shows a rotation model of the Earth where point p is the location of the gyro, whose latitude is α. The z-axis is defined along the normal line for the horizontal plane P at point p. The s-axis is defined on the horizontal plane with a deflection angle β from the meridian of point p. The z and s components ω_z and ω_s for the angular velocity of the Earth's rotation ω are expressed as:

$$\omega_z = \omega \cdot \sin\alpha \quad \ldots \ldots \ldots \ldots \quad (5)$$

and

$$\omega_s = \omega \cdot \cos\alpha \cdot \cos\beta, \quad \ldots \ldots \ldots \quad (6)$$

respectively.

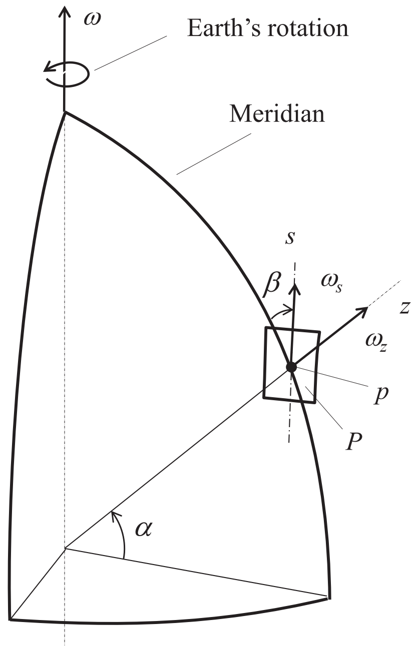

Fig. 2. Effects of the Earth's rotation.

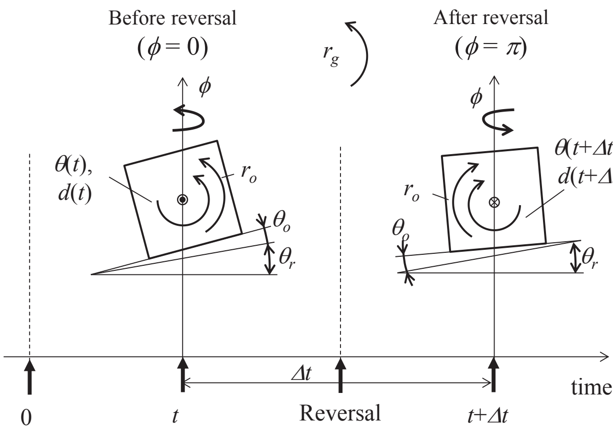

Fig. 3. Reversal measurements considering the effects of the Earth's rotation r_g and the gyro rate offset r_o.

Figure 3 shows an analysis model considering the effects of the Earth's rotation r_g together with the gyro rate offset r_o. The gyro rate offset is an offset for the angular velocity (rate) of the gyro and is comparable to r_g for fairly precise gyros.

The angles $\theta(t)$ and $\theta(t+\Delta t)$ detected by a gyro before and after reversal at times t and $t+\Delta t$ are expressed as:

$$\theta(t) = \theta_r + \theta_o + (r_o + r_g) \cdot t + d(t) \quad \ldots \ldots \quad (7)$$

and

$$\begin{aligned} \theta(t+\Delta t) = & -\theta_r + \theta_o + r_o(t+\Delta t) \cdot t \\ & + r_g(\Delta t - t) \cdot t + d(t+\Delta t), \quad \ldots \quad (8) \end{aligned}$$

respectively.

Here, the gyro drifts $d(t)$ and $d(t+\Delta t)$ consist of components except linear functions of t, because the linear component of the drift is included in the rate offset r_o and

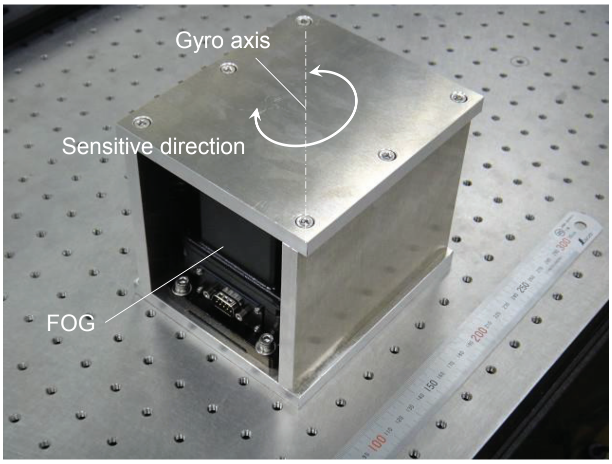

Fig. 4. FOG unit enclosed by four aluminum plates.

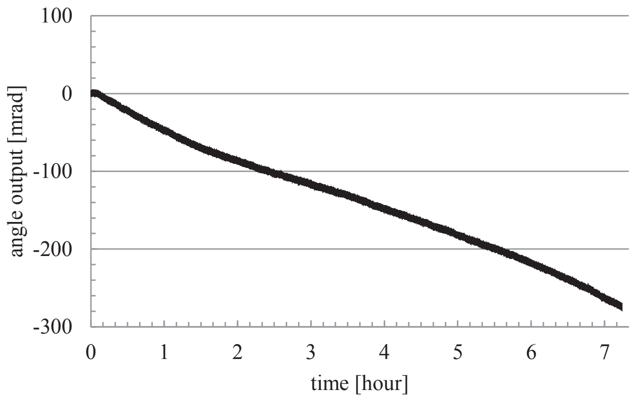

(a)

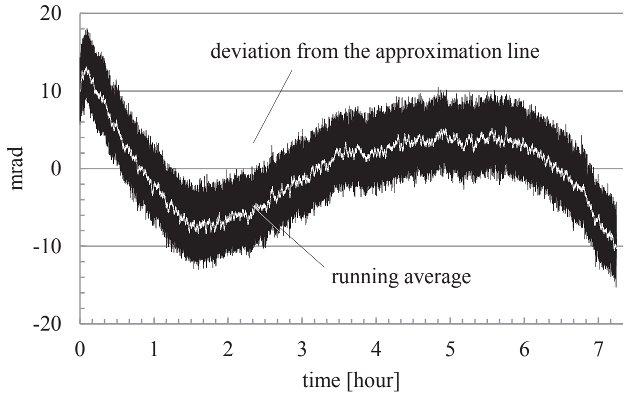

(b)

Fig. 5. (a) Drift of the angular output of the FOG unit and (b) Deviation from the approximation line.

the angle offset θ_o.

The angle of the object θ_r can be derived as:

$$\theta_r = \frac{\theta(t) - \theta(t+\Delta t)}{2} + \frac{(r_o + r_g)\cdot\Delta t}{2} - r_g \cdot t, \quad (9)$$

assuming that the reversal measurement is conducted at a sufficient rate, that is to say $d(t) \approx d(t+\Delta t)$.

If the location and direction of the gyro compared to the Earth were stable within each period of reversal, the effects of the Earth's rotation r_g would be constant. Then, the second term on the right hand side of Eq. (9) ($\{(r_o+r_g)\cdot\Delta t\}/2$) would be constant and would not affect the evaluated straightness because it is a slope component for the straightness. The third term, which is proportional to time t, can be compensated with the relations expressed in Eqs. (5) and (6), with known α and β, or by deriving r_g and r_o, as mentioned below.

3. Expermiments

We used a commercially available fiber optic gyro (FOG) unit, TA4265 N1510 (size: $65 \times 130 \times 85$ mm; mass: < 1.5 kg; range: ± 180 deg; operation cycle: 100 Hz; drift: 3 deg/h-rms; Tamagawa Seiki Co., Ltd.). It has one sensitive direction around the axis perpendicular to its bottom face. In this paper, we refer to this as the gyro axis. In order to use the gyro for detecting the angle around a horizontal axis, we enclosed the gyro in a four-sided aluminum box, as shown in **Fig. 4**.

All measurements described here were performed on an optical surface plate attached to a granite table in an air-conditioned room with a room temperature of 23 ± 1 deg.

3.1. Drift Measurements

We confirmed the stability of the gyro by monitoring an angle signal for a long period. The gyro was placed on the surface plate with its bottom face down, as shown in **Fig. 4**, where the gyro is sensitive for an angle around the vertical axis.

Figure 5(a) shows an angle signal as a function of time, which expresses the drift of the FOG unit. **Fig. 5(b)** shows a deviation from its least squares approximation line, which is the drift $d(t)$ and $d(t+\Delta t)$ to be eliminated in Eqs. (7) and (8). It has a high frequency component with a width of approximately ± 5 mrad, which can be eliminated by low pass filtering. The remaining lower frequency component is the target to be eliminated by the reversal measurement. **Fig. 5(b)** also shows a simple running average for the deviation, which corresponds to the lower frequency component to be eliminated. It is estimated to be several mrad/h after 2 hours of warming up and is expected to be reduced to several μrad/s by adopting the appropriate low pass filter.

3.2. Reversal Measurements

We performed reversal measurements in order to confirm their potential for eliminating the gyro drift. The gyro was set on the surface plate with its side facing down, as shown in **Fig. 6**, where the gyro has angle sensitivity around the horizontal axis.

The latitude of the gyro α was 36 deg, and the deflection angle β of the gyro's sensitive axis was 5 deg from the meridian. The reversal measurement was done manually with an interval Δt of 60 s. The side face of the enclo-

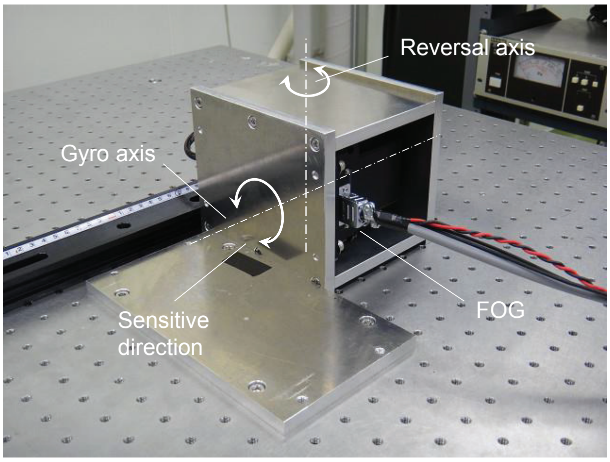

Fig. 6. Setup for the reversal measurement.

Table 1. Experimental conditions.

α	Latitude of the gyro	36 deg
β	Deflection angle of the gyro sensitive axis from the meridian	5 deg
Δt	Reversal interval	60 s
ω	Angular velocity (rate) of the Earth's rotation	73 μrad/s

sure maintained constant contact with the surface plate to avoid unnecessary angular change in the sensitive direction of the gyro. The experimental conditions are summarized in **Table 1**.

Figure 7 shows the angle detected by the gyro for the successive 60 reversal measurements performed over about an hour.

4. Discussion

The differences between the angles detected before and after reversal:

$$\theta(t)-\theta(t+\Delta t)=2\theta_r-(r_o+r_g)\cdot\Delta t+2r_g\cdot t \\ +d(t)-d(t+\Delta t) \quad . \quad . \quad . \ (10)$$

and

$$\theta(t+\Delta t)-\theta(t+2\Delta t)=-2\theta_r-(r_o-r_g)\cdot\Delta t-2r_g\cdot t \\ +d(t+\Delta t)-d(t+2\Delta t) \quad . \ . \ . \ . \ . \ . \ . \ . \ (11)$$

are derived from Eqs. (7) and (8). They indicate that the angular velocity caused by the Earth's rotation r_g can be derived from their time-proportional components $2r_g\cdot t$ and $-2r_g\cdot t$ because the drift terms $d(t)$, $d(t+\Delta t)$, and $d(t+2\Delta t)$ in Eqs. (10) and (11) are defined without the timeproportional component.

On the other hand, the difference between the angles detected one reversal cycle apart:

$$\theta(t)-\theta(t+2\Delta t)=-2\Delta t\cdot r_o+d(t) \\ -d(t+2\Delta t) \quad . \ . \ . \ . \ . \ (12)$$

is also derived from Eqs. (7) and (8). This indicates that the rate offset of the gyro r_o can be derived from its offset component $-2\Delta t\cdot r_o$ because the drift terms $d(t)$ and $d(t+2\Delta t)$ in Eq. (12) are also defined without the time-constant component.

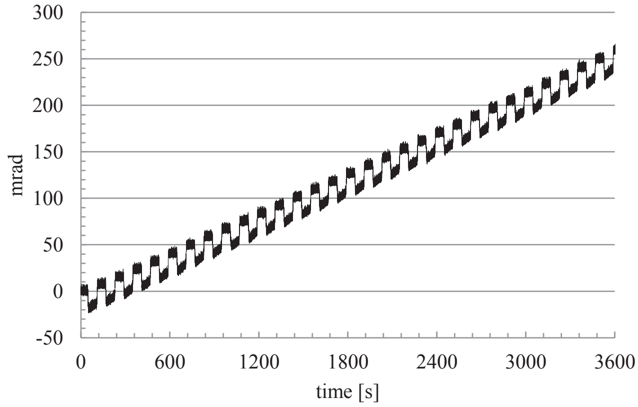

Fig. 7. Angle detected by the gyro for 60 reversal measurements.

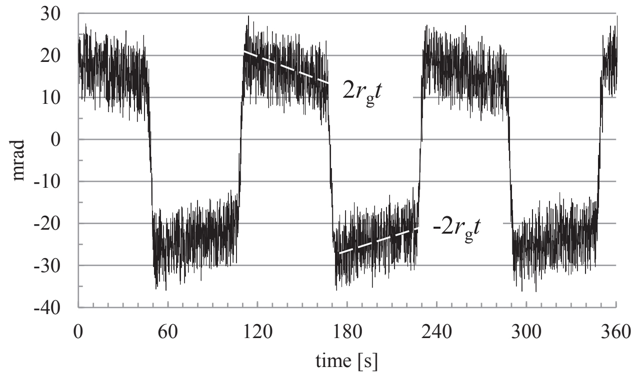

Fig. 8. $\theta(t)-\theta(t+\Delta t)$ derived from the measurements.

Figure 8 shows the differences between the angles detected before and after the reversal $\theta(t)-\theta(t+\Delta t)$ and $\theta(t+\Delta t)-\theta(t+2\Delta t)$, which is derived from the measurements expressed by **Fig. 7**. The slopes of each upper and lower side, expressed by dashed lines in **Fig. 8**, express $2r_g\cdot t$ and $-2r_g\cdot t$, respectively. It follows that the effects of the Earth's rotation r_g can be derived to be -55 ± 15 μrad/s, where 15 μrad/s is the standard deviation for each reversal. This is similar to 59 μrad/s derived from the relation expressed by Eq. (6) using the measurement conditions, where the altitude $\alpha=36$ deg and the deflection angle $\beta=5$ deg. The difference in the plus/minus sign between these values is caused by the definition of the experimental coordinates.

Figure 9 shows the difference between the angles detected one cycle apart $\theta(t)-\theta(t+2\Delta t)$, which is also derived from the measurements expressed by **Fig. 7**. The offset of the graph, expressed by the dashed line in **Fig. 9**, corresponds to $-2\Delta t\cdot r_o$. It follows that the rate offset of the gyro r_o can be derived to be 61 ± 39 μrad/s, where 39 μrad/s is the standard deviation for each reversal.

Figure 10 shows the angle of the object θ_r to be detected. It was obtained by substituting the derived r_g and r_o into the relation expressed in Eq. (9). The angle

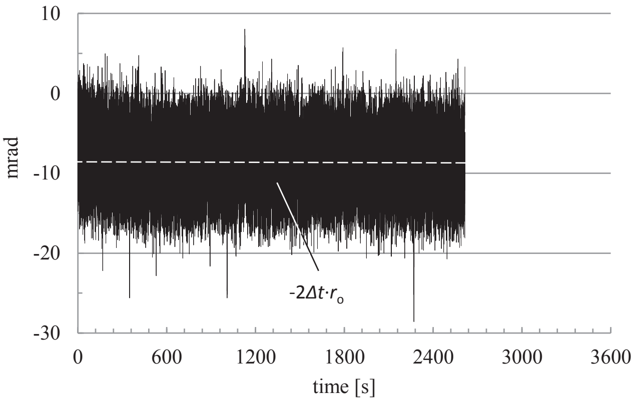

Fig. 9. $\theta(t) - \theta(t+2\Delta t)$ derived from the measurements.

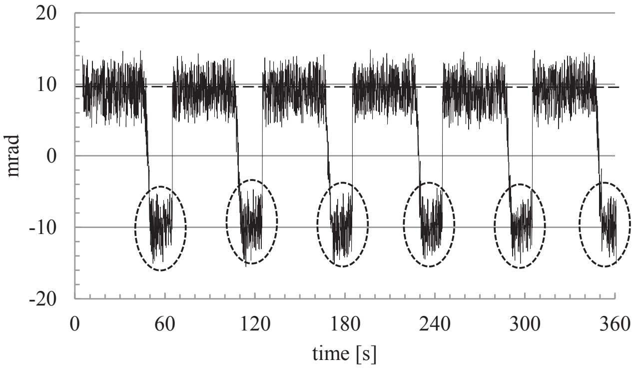

Fig. 10. θ_r derived from the measurements.

was derived to be 9.1 ± 0.4 mrad, where 0.4 mrad is the standard deviation for all of the measurements performed over about an hour. Considering that the gyro drift to be eliminated is several mrad/h (cf. **Fig. 5(b)**), this expresses that the reversal measurement is effective for reducing the effects of the gyro drift. The periodical dips shown in **Fig. 10** circled by dotted lines seem to be spurious by the transition in each reversal.

The results derived from the experiment are summarized in **Table 2**.

5. Conclusions

We considered adopting the reversal measurement for eliminating the gyro drift in order to realize a straightness evaluation based on tangential angle detection without being affected by gravity.

We used a commercially available FOG unit (size: $65 \times 130 \times 85$ mm; mass: < 1.5 kg) for evaluating the validity of the reversal measurements in reducing the gyro drift. The drift to be eliminated was measured and estimated to be several mrad/h from the measurement.

We periodically performed reversal measurements with an interval of 60 s and derived an angle with a standard deviation of 0.4 mrad for all of the measurements performed over about an hour. This indicates that the reversal measurement is effective in reducing the effects of the several mrad/h of gyro drift.

Table 2. Experimental results.

r_g	Effect of the Earth's rotation	-55 ± 15 μrad/s
r_o	Gyro rate offset	61 ± 39 μrad/s
θ_r	Angle of the object	9.1 ± 0.4 mrad

Acknowledgements

The authors thank K. Harada of the Accelerator Laboratory at KEK for providing instruments for experiments. The authors also thank Prof. M. Yamanaka and members in Mechanical Engineering Center at KEK for encouraging and supporting our studies. This work was supported by Collaborative Development Research Program of KEK (2014-ARL-2) and JSPS KAKENHI Grant Number 25420077.

References:

[1] I. Abe , N. Akasaka, M. Akemoto, S. Anami, A. Enomoto, et al., "The KEKB injector linac," Nuclear Instruments and Methods A499, 167, 2003.
[2] http://www-superkekb.kek.jp/ [accessed Dec. 26, 2014]
[3] http://j-parc.jp/index-e.html [accessed Dec. 26, 2014]
[4] http://xfel.riken.jp/eng/index.html [accessed Dec. 26, 2014]
[5] http://home.web.cern.ch/topics/large-hadron-collider [accessed Dec. 26, 2014]
[6] http://www.linearcollider.org/ILC [accessed Dec. 26, 2014]
[7] W. B. Herrmannsfeldt, M. J. Lee, J. J. Spranza, and K. R. Trigger, "Precision Alignment Using a System of Large Rectangular Fresnel Lenses," Appl. Opt., Vol.7, 995, 1968.
[8] D. Kämtner and J. Prenting, "Straight Line Reference System (SLRS) for the Adjustment of the X-Ray Free-Electron Laser (XFEL) at DESY," the 9th International Workshop on Accelerator Alignment (IWAA2006), Menro Park CA USA, September 25-29, 2006.
[9] H. M. Durand, M. Anastasopoulos, S. Griffet, J. Kemppinen, V. Rude, and M. Sosin, "Validation of the CLIC Alignment Strategy on Short Range," the 12th International Workshop on Accelerator Alignment (IWAA2012), Batavia IL USA, September 10-14, 2012.
[10] http://www-conf.slac.stanford.edu/iwaa/default.htm [accessed Dec. 26, 2014]
[11] T. Suwada, M. Satoh, S. Telada, and K. Minoshima, "Propagation and Stability Characteristics of a 500-m-long Laser-based Fiducial Line for High-precision Alignment of Long-distance Linear Accelerators," Rev. Sci. Instrum., Vol.84, 093302, 2013.
[12] W. T. Estler, K. L. Edmundson, G. N. Peggs, and D. H. Parker, "Large-Scale Metrology – An Update," CIRP Annals-Manufactureing Technology, Vol.51, No.2, 587, 2002.
[13] F. Franceschini, M. Galetto, D. Maisano, L. Mastrogiacomo, and B. Pralio, "Distributed Large-ScaleDimensional Metrology," Springer.
[14] A. E. Ennos and M. S. Virdee, "High Accuracy Profile Measurement of Quasi-conical Mirror Surfaces by laser autocollimation," Prec. Eng., Vol.4, No.5, 1982.
[15] G. Makosch and B. Drollinger, "Surface Profile Measurement with a Scanning Differential AC Interferometer," Appl. Opt., Vol.23, 4544, 1984.
[16] J. Yellowhair and J. H. Burge, "Analysis of a Scanning Pentaprism System for Measurements of Large Flat Mirrors," Appl. Opt., 46, Vol.35, 8466, 2007.
[17] J. Yellowhair and J. H. Burge, "Measurement of Optical Flatness Using Electronic Levels," Opt. Engineering, Vol.47, No.2, 023604, 2008.
[18] S. G. Alcock, K. J. S. Sawhney, S. Scott, U. Pedersen, R. Walton, F. Siewert, T. Zeschke, F. Senf, T. Noll, and H. Lammert, "The Diamond-NOM:A Non-contact Profiler Capable of Characterizing Optical Figure Error with Sub-nanometre Repeatability," Nuclear Instruments and Methods A616, pp. 224-228, 2010.
[19] K. Ishikawa, T. Takamura, M. Xiao, S. Takahashi, and K. Takamasu, "Profile Measurement of Aspheric Surfaces Using Scanning Deflectometry and Rotating Autocollimator with Wide Measuring range," Meas. Sci. Technol., Vol.25, 064008, 2014.
[20] T. Kume, E. Okuyama, M. Satoh, T. Suwada, and K. Furukawa, "Large-scale Accelerator Alignment Using an Inclinometer," Precision Engineering, Vol.37, pp. 825-830, 2013.

[21] T. Kume, M. Satoh, T. Suwada, K. Furukawa, and E. Okuyama, "Straightness evaluation using inclinometers with a pair of offset bars," Precision Engineering, Vol.39, pp. 173-178, 2015.
[22] C. J. Evans, R. J. Hocken, and W. T. Estler, "Self-calibration: reversal, redundancy, errorseparation, and 'Absolute testing'," CIRP Annual Manufacturing Technology, Vol.45, pp. 617-634, 1996.

Name:
Tatsuya Kume

Affiliation:
Mechanical Engineering Center, High Energy Accelerator Research Organization (KEK)

Address:
1-1 Oho, Tsukuba, Ibaraki 305-0801, Japan

Brief Biographical History:
1989 Joined Nippon Telegraph and Telephone Corp (NTT)
2002 Joined High Energy Accelerator Research Organization (KEK)

Main Works:
- "Straightness evaluation using inclinometers with a pair of offset bars," Precision Engineering, Vol.39, pp. 173-178, 2015.
- "Progress on the cryogenic system for the KAGRA cryogenic interferometric gravitational wave telescope," Class. Quantum Grav., Vol.31, 224003, 2014.
- "Analysis on effects of transverse electric field in an injector cavity of compact-ERL at KEK," Nucl. Instr. Meth., A753, pp. 97-104, 2014.
- "Experimental validation of a novel compact focusing scheme for future energy-frontier linear lepton colliders," PRL 112, 034802, 2014.
- "Cryogenic design of a superconducting solenoid for muonium hyperfine structure measurement," IEEE Transactions on Applied Superconductivity, Vol.23, No.3, 2013.

Membership in Academic Societies:
- Japan Society for Precision Engineering (JSPE)
- Particle Accelerator Society of Japan (PASJ)
- Japan Society of Applied Physics (JSAP)
- Institute of Electronics, Information and Communication Engineers (IEICE)

Name:
Masanori Satoh

Affiliation:
Associate Professor, Accelerator Laboratory, High Energy Accelerator Research Organization (KEK)

Address:
1-1 Oho, Tsukuba, Ibaraki 305-0801, Japan

Name:
Tsuyoshi Suwada

Affiliation:
Associate Professor, Accelerator Laboratory, High Energy Accelerator Research Organization (KEK)

Address:
1-1 Oho, Tsukuba, Ibaraki 305-0801, Japan

Academic Societies & Scientific Organizations:
- Physical Society of Japan (JPS)
- Particle Accelerator Society of Japan (PASJ)

Name:
Kazuro Furukawa

Affiliation:
Professor, Accelerator Laboratory, High Energy Accelerator Research Organization (KEK)

Address:
1-1 Oho, Tsukuba, Ibaraki 305-0801, Japan

Brief Career:
1986 Joined High Energy Accelerator Research Organization (KEK)

Selected Publications:
- "The KEKB injector linac," Prog. Theor. Exp. Phys. 2013, 03A002, 2013.
- "Accelerator control system at KEKB and the linac," Prog. Theor. Exp. Phys. 2013, 03A008, 2013.

Academic Societies & Scientific Organizations:
- Physical Society of Japan (JPS)
- Particle Accelerator Society of Japan (PASJ)
- Nuclear and Plasma Sciences Society (IEEE-NPSS)

Name:
Eiki Okuyama

Affiliation:
Professor, Faculty of Engineering and Resource, Akita University

Address:
1-1 Tegata gakuen-machi, Akita 010-8502, Japan

Brief Biographical History:
1985-1991 Assistant Researcher, Akita National College of Technology, Japan
1991-1996 Assistant Researcher, Akita University, Japan
1995 Visiting Fellow, University of Warwick, UK
1996-2015 Associate Professor, Akita University, Japan
2015- Professor, Akita University, Japan

Main Works:
- E. Okuyama, "Multi-probe Method for Straightness Profile Measurement Based on Least Uncertainty Propagation," Precision Engineering, Vol.34, No.1, pp. 49-54, 2010.

Membership in Academic Societies:
- Japan Society for Precision Engineering (JSPE)
- European Society for Precision Engineering and Nanotechnology (EUSPEN)